

Supporting Information

Title: Enzymatic X-ray Absorption Spectroelectrochemistry

Karolina Czastka,^a Alaa A Oughli,^b Olaf Rüdiger,^{a*} Serena DeBeer^{a*}

^a Max Planck Institute for Chemical Energy Conversion (MPI CEC), Stiftstraße 34-36, 45470 Mülheim an der Ruhr, Deutschland.

^b Technical University Munich, Campus Straubing for Biotechnology and Sustainability, Uferstraße 53, 94315 Straubing.

* Corresponding authors:

E-mail: serena.debeer@cec.mpg.de; olaf.ruediger@cec.mpg.de

Table of Contents

Methodology	4
Table S1. Selected parameters of beamlines where the experiments took place.	5
XAS flow-cell and setup employed for operando XAS studies performed in heterogeneous conditions .	7
Figure S1. Scheme of the gas-tight three-electrode PEEK custom-made spectroelectrochemical flow-cell used for operando XAS experiment in the hard X-ray regime, which consists of WE working electrode (GC plate), RE reference electrode, CE counter electrode.	7
Figure S2. Scheme of the experimental setup employed for operando XAS studies.	7
Figure S3. Schematic representation of enzyme/polymer film formation with Ni-SI _a [NiFe] cluster.	8
Ni K-edge XAS spectra of [NiFe] hydrogenase frozen reference solutions	9
Figure S4. The first derivative of Ni K-edge XAS spectra of [NiFe] hydrogenase from <i>DvMF</i> sample 1 (black line), 2 (red line) and 3 (blue line) measured at 10 K at SSRL beamline 9-3.....	10
Figure S5. Ni K-edge XAS spectra of [NiFe] hydrogenase from <i>DvMF</i> A) sample 1, B) 2, and C) 3 measured at one spot overtime at SSRL beamline 9-3 at 10 K. Each scan collected in 10 min.	11
Operando XAS studies of <i>DvMF</i> [NiFe] hydrogenase	12
Figure S6. Ni K-edge XAS spectra collected at 298 K at SAMBA Soleil beamline for a hydrogel film with [NiFe] hydrogenase from <i>DvMF</i> on GC electrode (black line), and upon OCP and phosphate electrolyte pH 7 saturated with H ₂ (green line).	12
Figure S7. Ni K-edge XAS spectra collected at 298 K at SAMBA Soleil beamline for a hydrogel film with [NiFe] hydrogenase from <i>DvMF</i> on GC electrode upon OCP and phosphate electrolyte pH 7 saturated with H ₂ (green line), and at $E = +200$ mV vs. SHE (blue line).....	13
Figure S8. Ni K-edge XAS spectra collected at 298 K at SAMBA Soleil beamline for a hydrogel film with [NiFe] hydrogenase from <i>DvMF</i> on GC electrode upon the flow of phosphate electrolyte pH 7 saturated with H ₂ at $E = +200$ mV (blue line), and at $E = -400$ mV vs. SHE (red line).....	14
Figure S9. Ni K-edge XAS spectra collected at 298 K at SAMBA Soleil beamline for a hydrogel film with [NiFe] hydrogenase from <i>DvMF</i> on GC electrode upon the flow of phosphate electrolyte pH 7 saturated with H ₂ at $E = -400$ mV (red line), and at $E = -150$ mV vs. SHE (violet line).	15
Figure S10. Ni K-edge XAS spectra collected at 298 K at SAMBA Soleil beamline for a hydrogel film with [NiFe] hydrogenase from <i>DvMF</i> on GC electrode upon the flow of phosphate electrolyte pH 7 saturated with H ₂ at $E = -150$ mV (violet line), and at $E = +200$ mV vs. SHE (dark cyan line).....	16
Figure S12. Ni K-edge XAS spectra collected at SAMBA beamline at Soleil at 298 K for [NiFe] hydrogenase hydrogel on GC electrode measured under +200 mV vs. SHE and H ₂ flow in phosphate buffer pH 7 overtime at the same spot. Collection time for one scan: A) 120 s, B) 300 s.	18
Figure S13. Ni K-edge XAS spectra collected at 298 K at the SAMBA beamline at Soleil for a hydrogel film with [NiFe] hydrogenase from <i>DvMF</i> on GC electrode upon the flow of phosphate electrolyte pH 7 saturated with H ₂ at +200 mV (cyan line), and at -400 mV vs. SHE (red line), and reference frozen solution of 1 (black line) and 3 (blue line) collected at SSRL beamline 9-3 at 10 K.....	19
Figure S14. Cyclic voltammogram (CV) of a GC electrode with a [NiFe] hydrogenase hydrogel in phosphate buffer pH 7 and H ₂ flow before (black line) and after (dark cyan line) X-ray operando	

measurements. Measured at room temperature and 20 mV/s of scan rate. The horizontal dashed line indicates a zero current. 20

Beam damage. Frozen reference samples vs. electrodes 21

Table S2. Fluence and flux density calculations for [NiFe] hydrogenase measured at 10 K at SSRL 9-3 (solutions) and at 298 K at Soleil SAMBA beamlines (film on GC electrodes) under the following conditions: the average flux of 10^{12} (phs⁻¹), 45° angle of incidence beam relative to the sample surface, TFY detection mode. 21

Methodology

Sample preparation. *Desulfovibrio vulgaris* Miyazaki F (*DvMF*) [NiFe] hydrogenase has been purified according to reported procedures.¹ A redox viologen-based polymer was synthesized and received as previously reported.² The following chemicals and materials were purchased (from Sigma Aldrich, unless otherwise indicated) and used as received: sodium dithionite (NaDT), Dipotassium phosphate (K_2HPO_4), Monopotassium phosphate (KH_2PO_4), and glassy carbon electrodes (GC, Hochtemperatur-Werkstoffe GmbH). Ultrapure water was obtained from the Millipore unit (18 M Ω cm) and used to prepare all aqueous solutions.

For reference XAS measurements, solutions of **1** [NiFe] hydrogenase *as isolated* in 0.1 M MES buffer pH = 6.5 (120 μ l, 0.91 mM), **2** [NiFe] hydrogenase (600 μ l, 0.91 mM in 0.1 M MES buffer pH = 6.5) flushed with 100% H₂ with a flow rate of 60 ml/min for 15 min, then incubated in H₂ atmosphere for 4 hours, and **3** [NiFe] hydrogenase (0.91 mM in 0.1 M MES buffer pH = 6.5) – 320 μ l mixed with 17 μ l viologen (31 mM) and 40 μ l NaDT (0.26 M) have been used. The sample preparation for **2** and **3** was carried out under anaerobic conditions in an inert atmosphere N₂ glovebox (MBraun LabMaster SP). Delrin XAS sample holders were filled with 120 μ l of [NiFe] hydrogenase reference samples (**1-3**) and frozen immediately in liquid nitrogen. All reference samples were characterized by FTIR.^{1, 3, 4}

FTIR spectroscopy. FTIR spectra were obtained using a Bruker IFS 66v/s FTIR spectrometer with a liquid-nitrogen-cooled photovoltaic mercury cadmium telluride detector element. Spectra were recorded with a 2.00 mm aperture, 1000 scans, and 2 cm⁻¹ resolution using the OPUS package (Bruker Optics). Data analysis was carried out with MATLAB script using KAZAN Viewer 2.1.4 developed by Boris Epel and Alexey Silakov. The IR bands have been assigned to redox states of *DvMF* [NiFe] hydrogenase based on previously reported FTIR characterization.^{1, 3, 4}

[NiFe] hydrogenase – viologen polymer film formation has been carried according to the reported procedure (SI, Figure S3).² 20 μ l of 0.4 mM *DvMF* [NiFe] hydrogenase (in 10 mM MES buffer pH 6.5) and 10 μ l of 33 mg/ml viologen-based polymer aqueous suspension were mixed and drop-casted on the GC electrode surface and left to dry. Next, 3 μ l of 0.1 M phosphate buffer pH 7 drop-casted on the enzyme-polymer film and covered with a watch glass to allowed the polymer hydrogel film formation for 30 min. Then, the electrode was left to dry for 1h.

Ni K-edge XAS measurements. Operando X-ray studies of [NiFe] hydrogenase entrapped in a redox viologen-based polymer matrix on GC electrode were conducted at the Soleil synchrotron facility at the SAMBA beamline (ring energy of 2.75 GeV, and ring current of 500 mA), using an operando custom-made spectroelectrochemical flow-cell (SI, Figure S1). Reference samples were measured at SSRL at beamline 9-3 (ring energy of 3.0 GeV, and ring current of 500 mA). At SAMBA, the energy was monochromatized using a sagittally focusing Si 220 monochromator. At SSRL beamline 9-3 a liquid N₂ cooled double-crystal monochromator with Si 220 crystals was used to select the incoming X-ray energy. All XAS scans were recorded by scanning the incident energy from 8.2 to 8.9 keV, using

fluorescence mode. A shutter, synchronized with the scanning program, was used to protect the sample from X-ray beam damage during optics movement. Additionally, a 0.25 mm Al filter was utilized to attenuate the incident beam and minimize beam induced sample damage. To minimize scattered X-rays in the fluorescence detector and improve the sample signal-to-noise ratio, a Co filter (3 mm thick) and Soller slit assembly were used. Reference samples were measured at 10 K in a liquid helium flow cryostat (SSRL 9-3), while Ni K-edge spectra collected under operando conditions have been measured at 298 K (Soleil SAMBA). In Table S1, the most important parameters for SSRL 9-3 and Soleil SAMBA beamlines are summarized. The absorption edge (E_0) was measured at the first inflection point in the derivative spectrum and calibrated vs. Ni foil to 8333.0 eV. Generally, using first derivatives is a more mathematically rigorous means to determine edge energies, however, in order to be consistent with previous reports, all energies of Ni K-edges within this project have been additionally determined at the position of a normalized edge at half-height.

No beam damage was observed upon consecutive measurements on any of the reference frozen samples at the reported conditions (SI, Figure S5). Presented data of frozen solutions of DvMF [NiFe] hydrogenase are merges of 5 scans, where each scan has been measured at different sample spots. Beam damage during operando XAS studies is also excluded by measuring consecutive edge scans, at the same sample spot. No changes in the spectra were observed for measuring times up to 3000 s (SI, Figure S11). Data presented in the operando XA-SEC section is an average of 15 Ni K-edge XAS scans under each CA step as presented in Figure 5 C where maximum 5 edge scans at the same spot have been collected.

For the XA-SEC experiments, the spectra were collected first on the dry enzyme-hydrogel film and then in the presence of the electrolyte saturated with H_2 . The [NiFe] hydrogenase was measured under H_2 oxidation conditions and while applying a negative potential to keep the viologen reduced. The stability of the system under turnover conditions was evaluated by following the electrocatalytic activity for H_2 oxidation, and the intensity of the spectra.

Table S1. Selected parameters of beamlines where the experiments took place.

Synchrotron	Beamline	Photon flux (ph/s)	Monochromator	Detector	Beam size (mm x mm; v x h)
SSRL	9-3	10^{12}	Si (220)	Canberra Ge 100 element	1 x 3
Soleil	SAMBA	10^{12}	Si (220)	Canberra Ge 35 element	1 x 0.5

Electrochemistry. All electrochemical measurements were carried out in anaerobic conditions using an operando custom-made spectroelectrochemical flow cell with a home-made gas-tight box where the buffer was saturated with H_2/N_2 gas mixtures (SI, Figure S1-

S2). Gas mixtures of H₂ and N₂ were controlled with mass flow controllers. Electrochemical experiments were controlled by AUTOLAB potentiostat. Ag|AgCl (3M KCl) was used as a reference electrode ($E_{\text{SHE}} = E_{\text{Ag|AgCl}} = + 181 \text{ mV}$ for Ag|AgCl |3M KCl reference electrode at 298 K). A Pt wire was used as a counter electrode and a 0.5 mm GC electrode as a working electrode. Herein, all potentials are converted vs. standard hydrogen electrode (SHE).

XAS flow-cell and setup employed for operando XAS studies performed in heterogeneous conditions

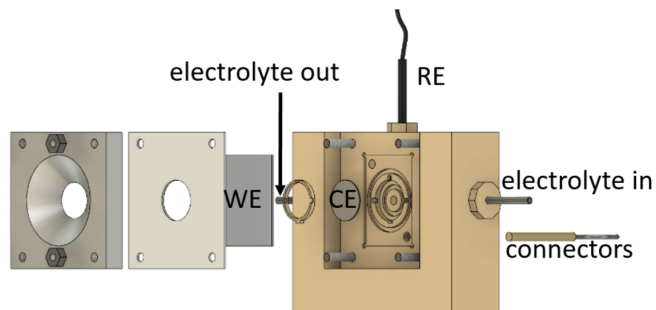


Figure S1. Scheme of the gas-tight three-electrode PEEK custom-made spectroelectrochemical flow-cell used for operando XAS experiment in the hard X-ray regime, which consists of WE working electrode (GC plate), RE reference electrode, CE counter electrode.

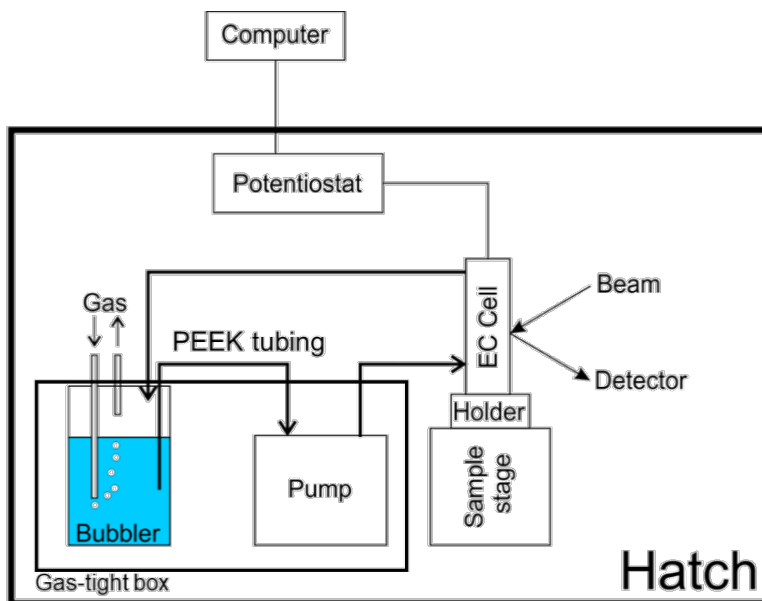


Figure S2. Scheme of the experimental setup employed for operando XAS studies.

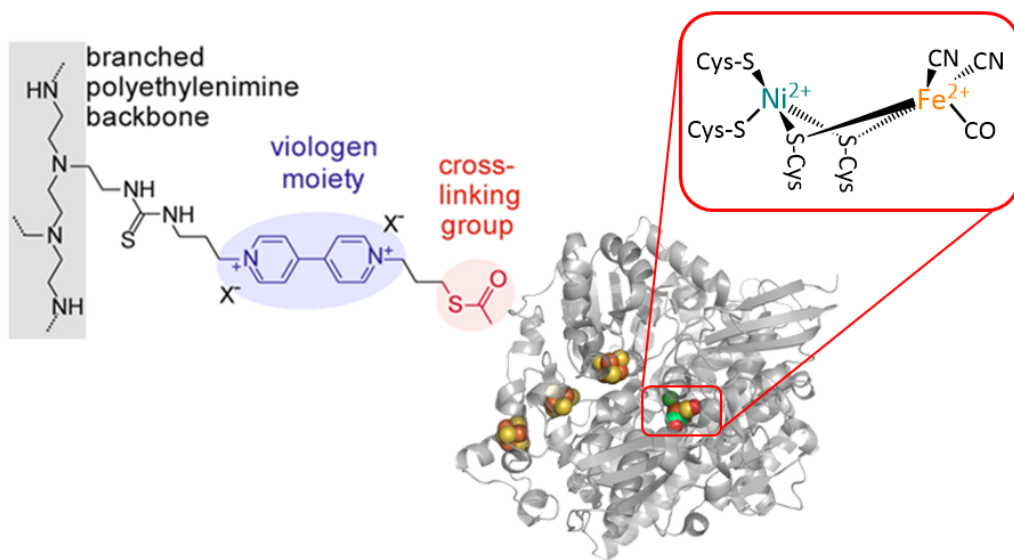
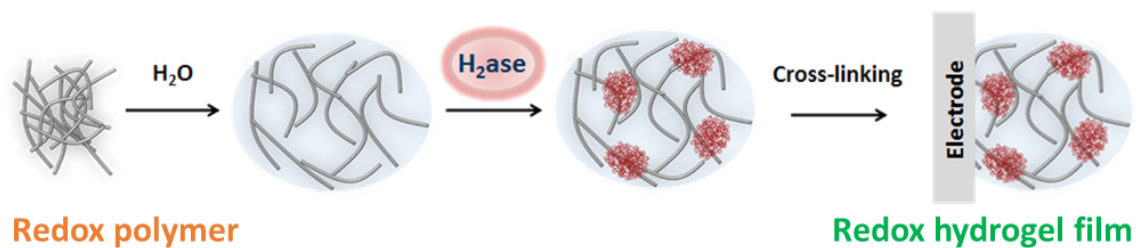


Figure S3. Schematic representation of enzyme/polymer film formation with Ni-SI_a [NiFe] cluster. Reprinted with permission from Plumeré et al., Nat. Chem. 2014.³

Ni K-edge XAS spectra of [NiFe] hydrogenase frozen reference solutions

The Ni K-edges spectra for all reference samples of [NiFe] hydrogenase (Figure 3, Table 2) show a weak pre-edge feature which is assigned to the $1s \rightarrow 3d$ transition. The $1s \rightarrow 3d$ pre-edge for **1** appears at 8331.9 eV, and the edge line appears at 8338.7 eV. The $1s \rightarrow 3d$ pre-edge and edge line in **2** are shifted about 0.4 eV to higher energies and displays a new feature at 8337 eV. This can be related to the local symmetry changes on the Ni site, where a D_{4h} symmetry is suggested based on previous studies on Ni model complexes for [NiFe] hydrogenase.⁵ An oxidation state assignment based on the rising edge line position is complicated for the sample reduced with H_2 due to the geometric and electronic changes that occur at the Ni center. For **1**, a trivalent with a five-coordinated Ni center organized in a distorted C_{4v} geometry is assumed (Table 1). The energy of the K-edge of sample **2** suggests a more oxidized Ni center than was observed for the **1**. Therefore, using the edge as a marker of oxidation state in this case is misleading (SI, Figure S4). The Ni K-edge spectrum for sample **3** shows changes in the edge shape (Figure 3). The Ni K-edge edge becomes sharper (edge marked with asterisk). Similar behaviour upon Ni-C formation has been reported for O_2 -sensitive [NiFe] hydrogenase from *Thiocapsa roseopersicina* (*Tr*) and O_2 -tolerant [NiFe] hydrogenase from *Ralstonia eutropha* (*Re*).^{6, 7} The Ni K-edge rising edge energy is at 8341.7 eV, which is about 2.6 eV higher in energies than enzyme incubated in H_2 atmosphere sample. This is consistent with an increased amount of Ni-C for the NaDT/viologen reduced sample (**3**) compared to the H_2 reduced sample (**2**, Table 1).

Recently, it was shown that the high degree of covalency between the Ni ion and the cysteine thiolate in metalloenzyme complexes complicates formal oxidation state assignments.⁸ In general, the presence of the sulfur ligands minimize edge shifts due to the strong covalent character.^{7, 9, 10} This is consistent with our Ni K-edge spectra, where Ni-B (**1**) and Ni-R (**2**) rich samples, containing cysteinyl thiolate ligands in C_{4v} and D_{4h} symmetry, respectively, display minimal K-edge energy shifts, and highlights the importance of careful analysis of the edge position when using it as a marker for determining the oxidation state. Ni K-edge XAS studies of reference sample indicate that subtle changes should be observed mainly in the edge region, and the analysis of data collected under turnover condition will be challenging due to geometry transformations, as well as changes in electronic configuration.

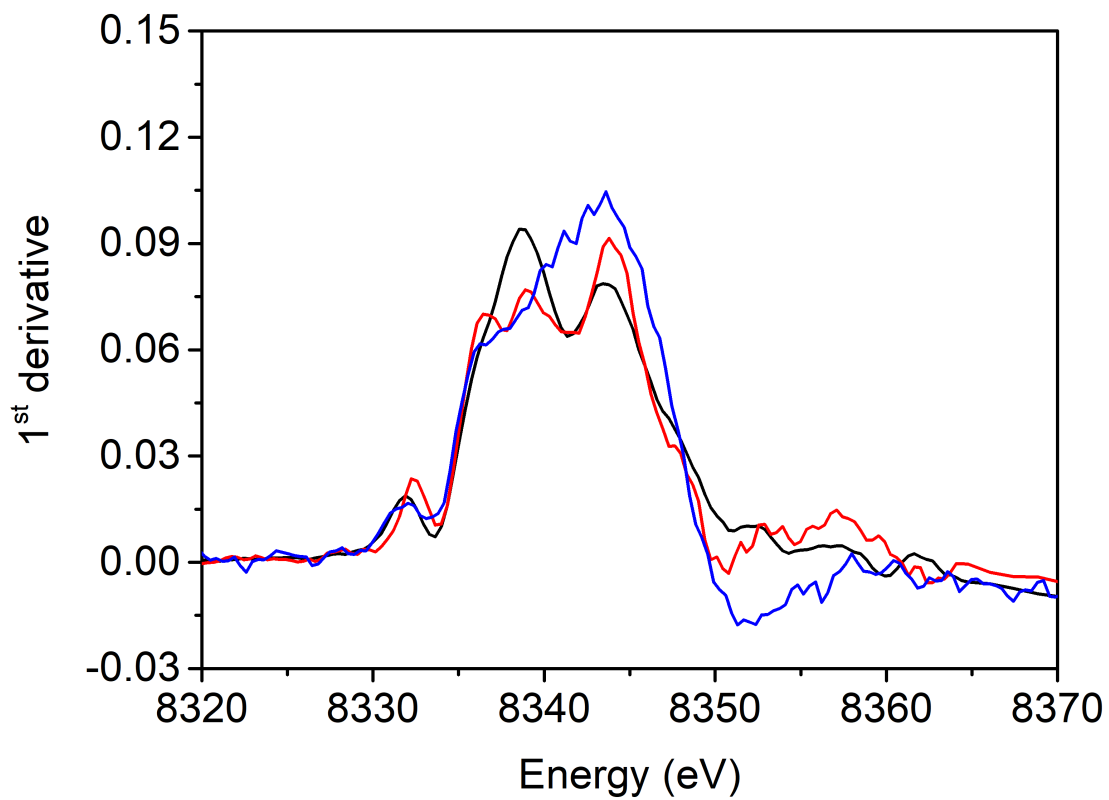


Figure S4. The first derivative of Ni K-edge XAS spectra of [NiFe] hydrogenase from *DvMF* sample **1** (black line), **2** (red line) and **3** (blue line) measured at 10 K at SSRL beamline 9-3.

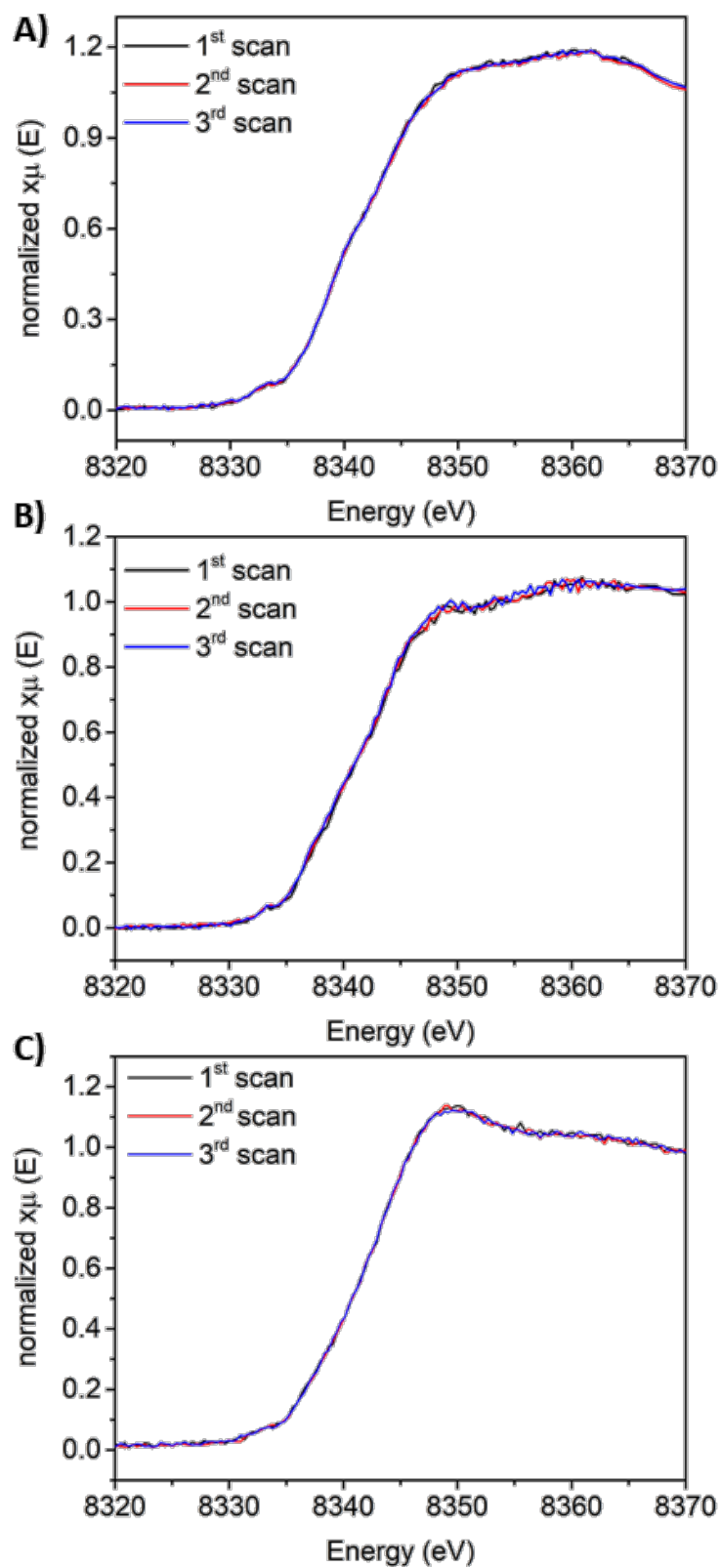


Figure S5. Ni K-edge XAS spectra of [NiFe] hydrogenase from *DvMF* A) sample 1, B) 2, and C) 3 measured at one spot overtime at SSRL beamline 9-3 at 10 K. Each scan collected in 10 min.

Operando XAS studies of *Dv*MF [NiFe] hydrogenase

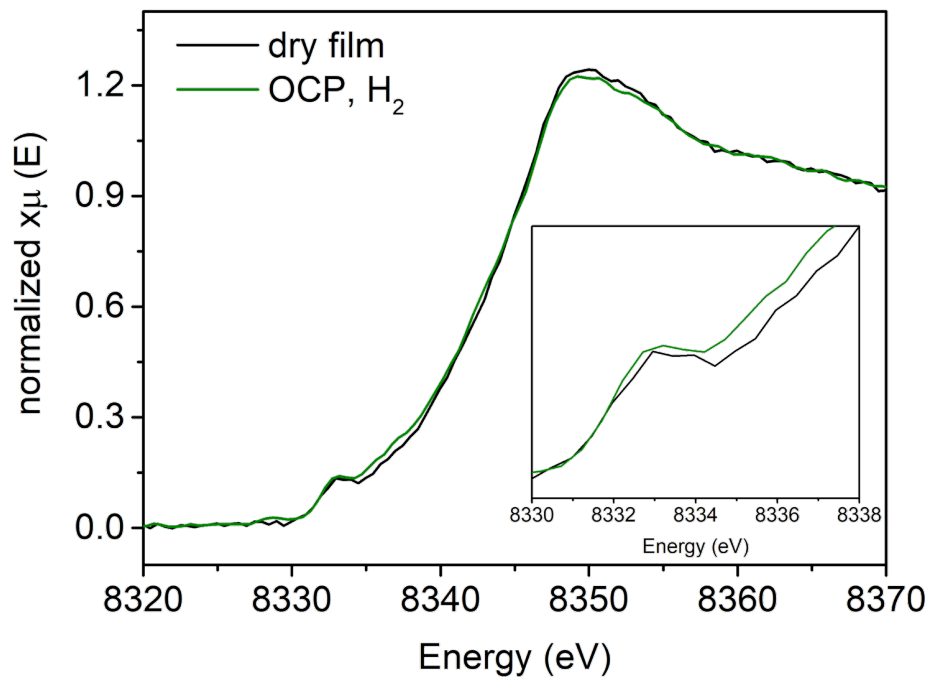


Figure S6. Ni K-edge XAS spectra collected at 298 K at SAMBA Soleil beamline for a hydrogel film with [NiFe] hydrogenase from *Dv*MF on GC electrode (black line), and upon OCP and phosphate electrolyte pH 7 saturated with H₂ (green line).

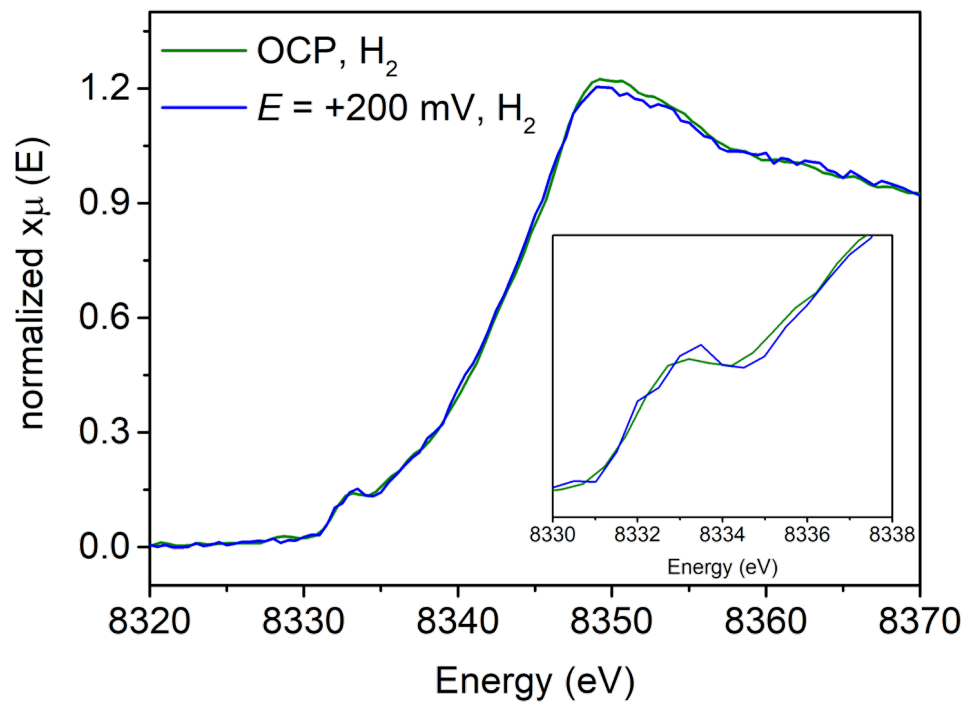


Figure S7. Ni K-edge XAS spectra collected at 298 K at SAMBA Soleil beamline for a hydrogel film with [NiFe] hydrogenase from *DvMF* on GC electrode upon OCP and phosphate electrolyte pH 7 saturated with H₂ (green line), and at $E = +200$ mV vs. SHE (blue line).

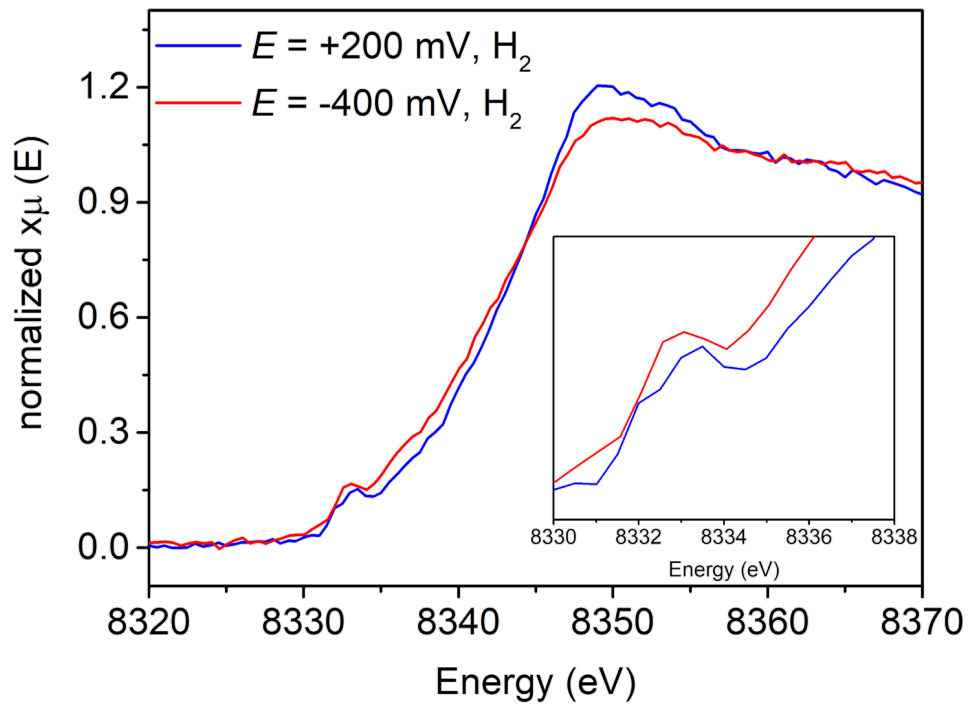


Figure S8. Ni K-edge XAS spectra collected at 298 K at SAMBA Soleil beamline for a hydrogel film with [NiFe] hydrogenase from *DvMF* on GC electrode upon the flow of phosphate electrolyte pH 7 saturated with H_2 at $E = +200$ mV (blue line), and at $E = -400$ mV vs. SHE (red line).

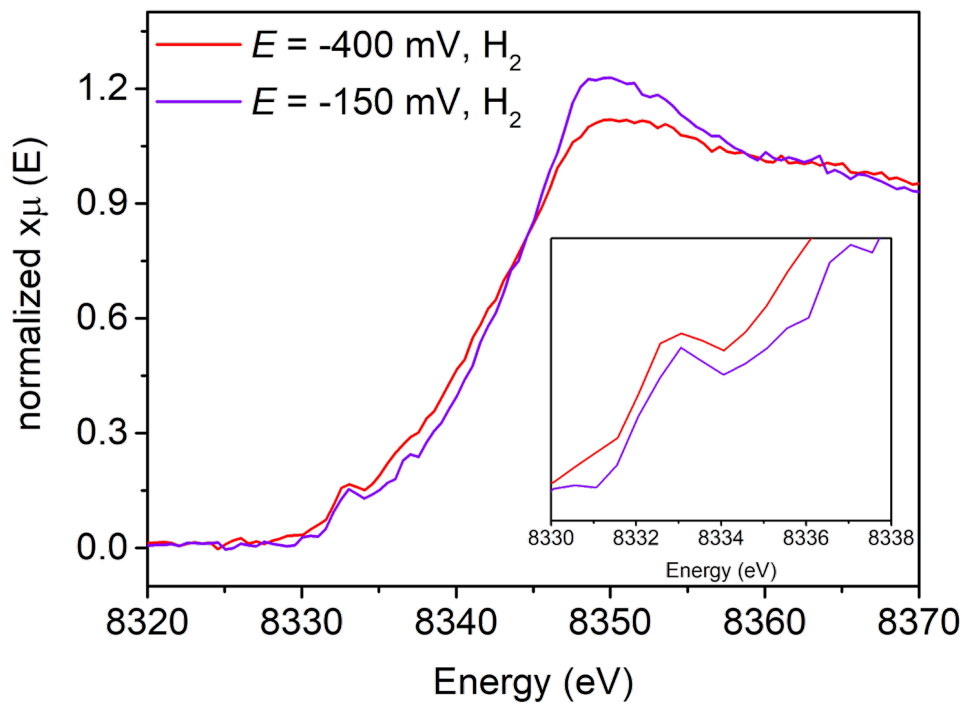


Figure S9. Ni K-edge XAS spectra collected at 298 K at SAMBA Soleil beamline for a hydrogel film with [NiFe] hydrogenase from *DvMF* on GC electrode upon the flow of phosphate electrolyte pH 7 saturated with H_2 at $E = -400$ mV (red line), and at $E = -150$ mV vs. SHE (violet line).

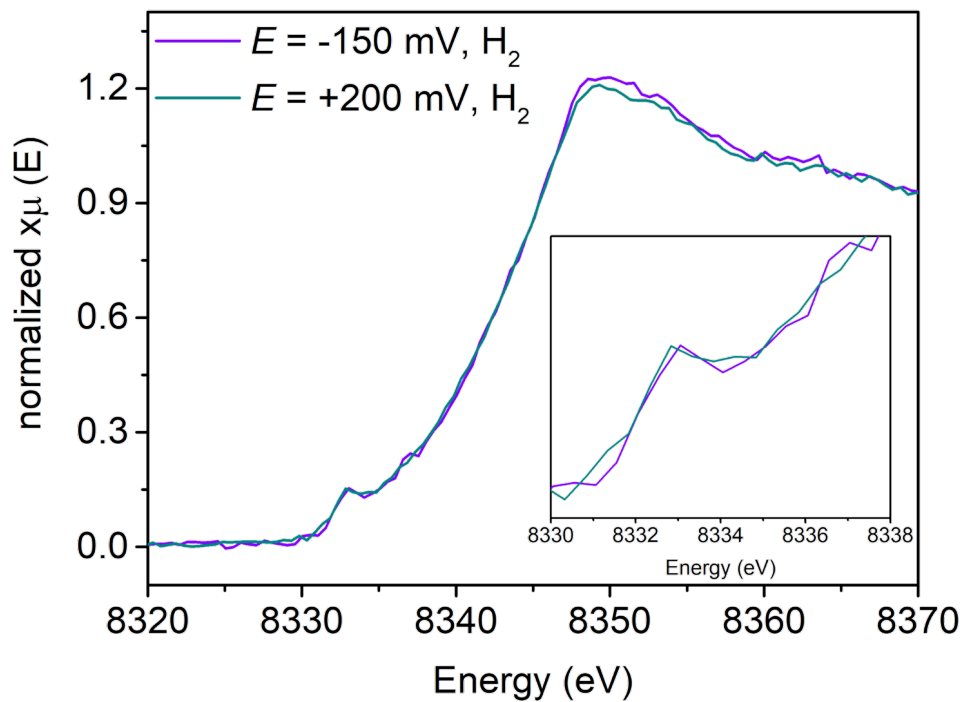


Figure S10. Ni K-edge XAS spectra collected at 298 K at SAMBA Soleil beamline for a hydrogel film with [NiFe] hydrogenase from *DvMF* on GC electrode upon the flow of phosphate electrolyte pH 7 saturated with H_2 at $E = -150 \text{ mV}$ (violet line), and at $E = +200 \text{ mV}$ vs. SHE (dark cyan line).

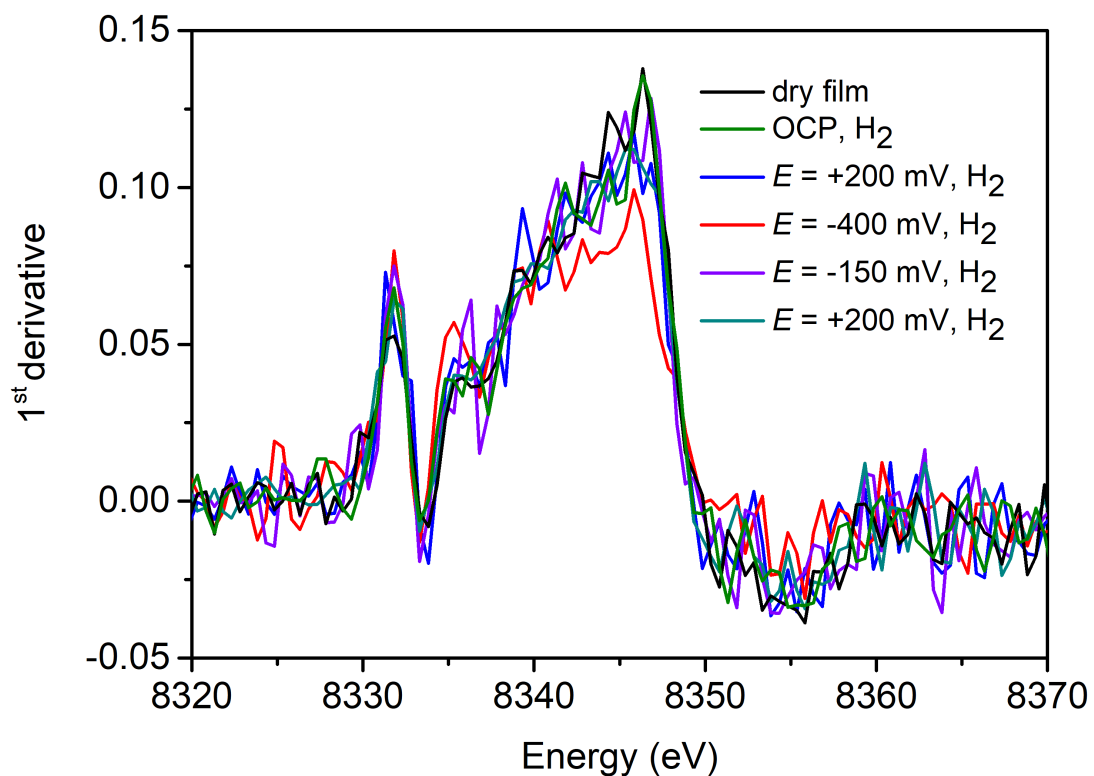


Figure S11. The first derivative of Ni K-edge XAS spectra of [NiFe] hydrogenase from *DvMF* on GC electrode dry film (black line), and measured, upon the flow of phosphate electrolyte pH 7 saturated with H_2 and OCP (green line), at $E = +200$ mV (blue line), at $E = -400$ mV (red line), at $E = -150$ mV (violet line), at $E = +200$ mV vs. SHE (dark cyan line).

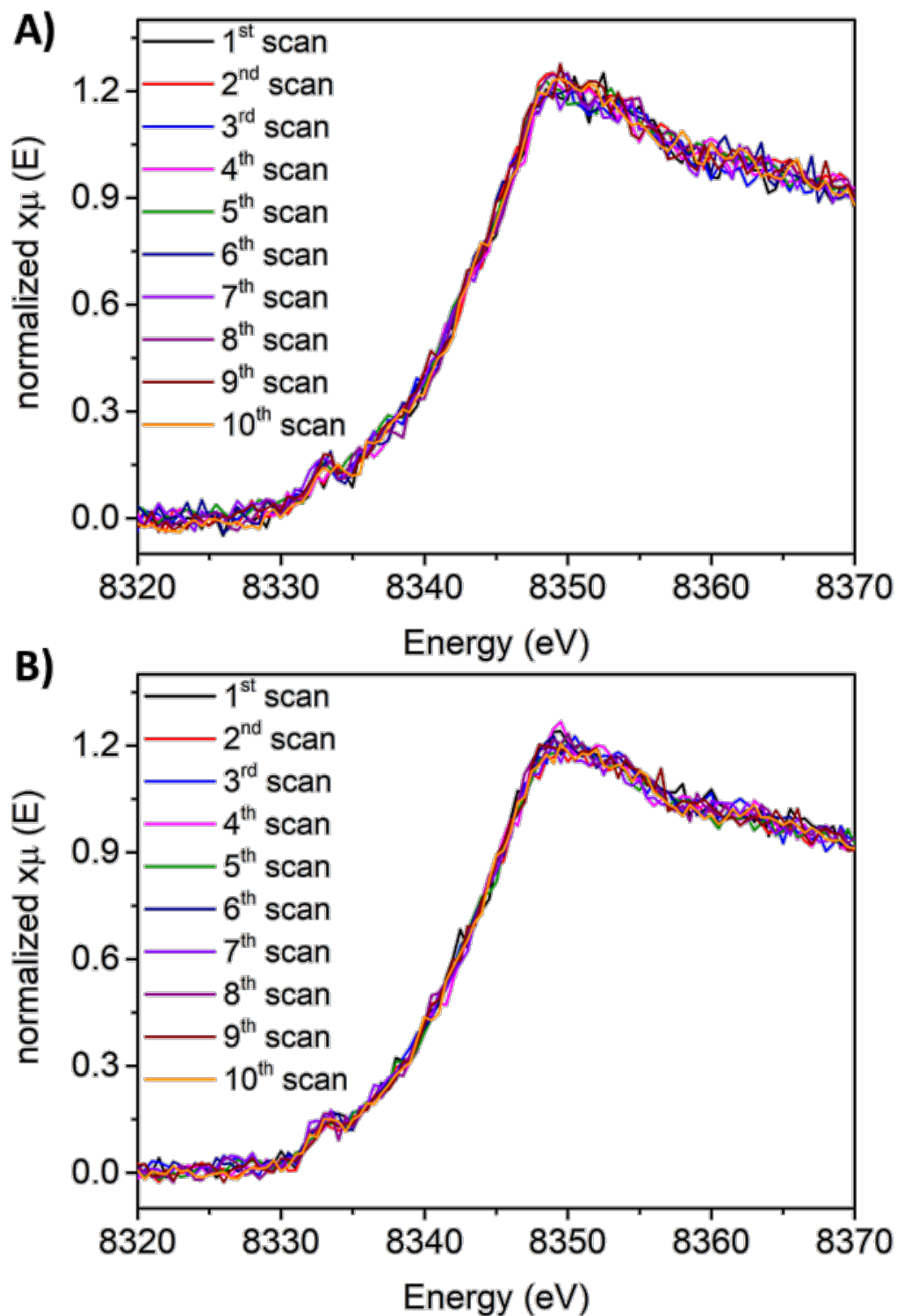


Figure S12. Ni K-edge XAS spectra collected at SAMBA beamline at Soleil at 298 K for [NiFe] hydrogenase hydrogel on GC electrode measured under +200 mV vs. SHE and H₂ flow in phosphate buffer pH 7 overtime at the same spot. Collection time for one scan: **A)** 120 s, **B)** 300 s.

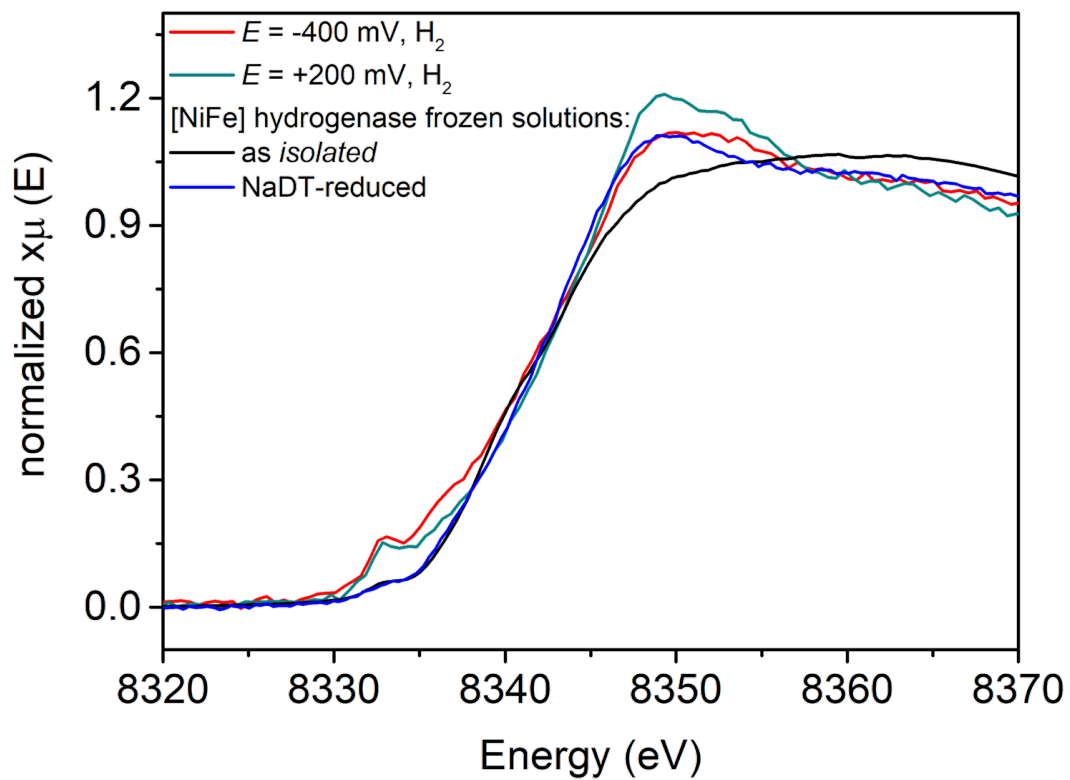


Figure S13. Ni K-edge XAS spectra collected at 298 K at the SAMBA beamline at Soleil for a hydrogel film with [NiFe] hydrogenase from *DvMF* on GC electrode upon the flow of phosphate electrolyte pH 7 saturated with H_2 at +200 mV (cyan line), and at -400 mV vs. SHE (red line), and reference frozen solution of **1** (black line) and **3** (blue line) collected at SSRL beamline 9-3 at 10 K.

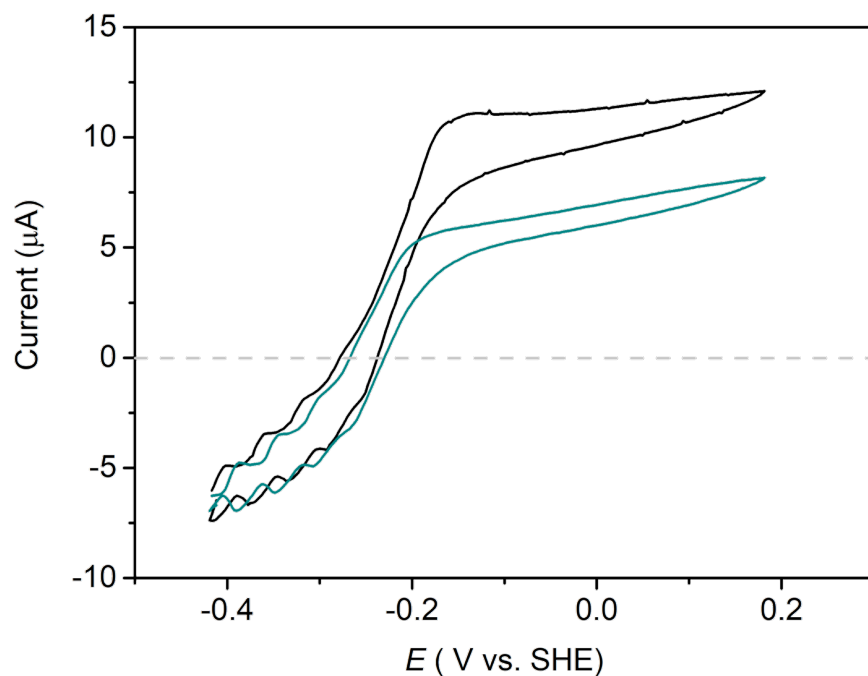


Figure S14. Cyclic voltammogram (CV) of a GC electrode with a [NiFe] hydrogenase hydrogel in phosphate buffer pH 7 and H₂ flow before (black line) and after (dark cyan line) X-ray operando measurements. Measured at room temperature and 20 mV/s of scan rate. The horizontal dashed line indicates a zero current.

The CV scan after operando XA-SEC studies indicate that around 70% of catalytic H₂ oxidation current was conserved.

Beam damage. Frozen reference samples vs. electrodes

To compare the conditions that the XAS data were collected at different synchrotron facilities, fluence and flux density parameters have been calculated. Fluence is referred to as a number of accumulated photons per area, while flux density accounts for the fluence per second.¹¹ Table S2 shows a fluence correlation for [NiFe] hydrogenase reference samples and [NiFe] hydrogenase-polymer-modified electrode measured at two different beamlines. It can be seen that flux density, depends strongly on the beam size, where lowering beam size by about one order of magnitude yields an order higher beam dose in area unit per seconds. Furthermore, it is shown that the fluence parameter increases linearly with exposure time in a given experiment and it is consistent with the observations reported in the literature.¹¹ Moreover it was show, that the concentration of the sample has a strong influence on the amounts of the accumulated photons in a data set, where one order lower concentrated sample is obtaining one order of magnitude higher radiation dose. Therefore, a skin dose that corresponds to the energy deposited in a volume set by a beam size and attenuation length (the depth into a material, measured along the surface) can be estimated. The reference [NiFe] hydrogenase samples are in a concentration range of 0.77 - 0.91 mM, which gives skin dose of 3.19×10^{-3} MGy. The enzyme-polymer-modified electrode yields similar range of concentration, however due to lower beam size the skin dose should be slightly higher i.e. ca. 9.56×10^{-3} MGy (in this case it is assumed that the concentration of the enzyme deposited on the electrode surface is similar to the reference frozen solution within all electrode area). The electrode coverage with [NiFe] hydrogenase has been reported to be about 1 pmol/cm² therefore estimated skin dose exposed within 1s is estimated to be nine orders higher. Hence, data collection for [NiFe] hydrogenase monolayer with the experimental conditions of at SAMBA beamline, would be extremely challenging due to requirement of longer time of sample irradiation with the beam to obtain satisfactory signal-to-noise ratio, which would increase probability of sample beam damage.

Table S2. Fluence and flux density calculations for [NiFe] hydrogenase measured at 10 K at SSRL 9-3 (solutions) and at 298 K at Soleil SAMBA beamlines (film on GC electrodes) under the following conditions: the average flux of 10^{12} (ph s⁻¹), 45° angle of incidence beam relative to the sample surface, TFY detection mode.

Beamline	Beam spot size ($\mu\text{m} \times \mu\text{m}$)	Exposure time (s)	Fluence (ph μm^{-2})	Flux density (ph s ⁻¹ μm^{-2})
SSRL 9-3	1000 x3000	600	2.0×10^8	3.3×10^5
Soleil Samba	1000 x 500	300	6.0×10^8	2.0×10^6

Within this report, we presented spectra collected for an enzyme with one given absorbing atom. For a 0.91 mM concentration of the protein in solution and a beam size of 1 mm x 3 mm (v x h), 1.81×10^{15} Ni atoms would be sampled within 1 mm depth, which results in total 17736 counts/second being detected. Monolayers of the protein on the electrode surface result in extremely low concentration, where about 5×10^9 Ni atoms could be probed using beam size of 1 mm x 3 mm. Consequently, since the absorbance is proportional to the sample concentration, the time for collecting enough photons to obtain acceptable signal-to-noise ratio increases by six orders of magnitude, resulting in approximately 1 count every 10 seconds. This is thus a signal that is unlikely to be detectable above background and even in cases where it could be would result in prohibitively long measurement times (of several weeks or longer). This suggests that XA-SEC measurements for protein monolayers are currently not feasible. For the enzyme-polymer film, the exact thickness of the film is difficult to estimate however the recorded counts per second can be utilized to estimate an effective concentration. We recorded 613 counts/sec for an enzyme-polymer film, which indicates an effective concentration of about 30 micromolar. This gives 1.0×10^{13} Ni atoms that are sampled with beam size of 1 mm x 0.5 mm (v x h). Hence, the estimated time to obtain an acceptable signal-to-noise ratio is about 30 times longer than what was required for reference frozen solution. These estimates indicate that the XA-SEC experiments are feasible, albeit challenging, for protein-polymer films.

References

1. C. Fichtner, C. Laurich, E. Bothe and W. Lubitz, *Biochemistry*, 2006, **45**, 9706-9716.
2. T. Yagi, K. Kimura, H. Daidoji, F. Sakai, S. Tamura and H. Inokuchi, *Journal of Biochemistry*, 1976, **79**, 661-671.
3. N. Plumeré, O. Rüdiger, A. A. Oughli, R. Williams, J. Vivekananthan, S. Pöller, W. Schuhmann and W. Lubitz, *Nat Chem*, 2014, **6**, 822-827.
4. M. E. Pandelia, H. Ogata, L. J. Currell, M. Flores and W. Lubitz, *Biochim. Biophys. Acta - Bioenergetics*, 2010, **1797**, 304-313.
5. S. Hugenbruch, H. S. Shafaat, T. Krämer, M. U. Delgado-Jaime, K. Weber, F. Neese, W. Lubitz and S. DeBeer, *Physical Chemistry Chemical Physics*, 2016, **18**, 10688-10699.
6. Z. Gu, J. Dong, C. B. Allan, S. B. Choudhury, R. Franco, J. J. G. Moura, I. Moura, J. LeGall, A. E. Przybyla, W. Roseboom, S. P. J. Albracht, M. J. Axley, R. A. Scott and M. J. Maroney, *Journal of the American Chemical Society*, 1996, **118**, 11155-11165.
7. M. Haumann, A. Porthun, T. Buhrke, P. Liebisch, W. Meyer-Klaucke, B. Friedrich and H. Dau, *Biochemistry*, 2003, **42**, 11004-11015.
8. E. C. Kisgeropoulos, A. C. Manesis and H. S. Shafaat, *Journal of the American Chemical Society*, 2021, **143**, 849-867.
9. G. J. Colpas, M. J. Maroney, C. Bagyinka, M. Kumar, W. S. Willis, S. L. Suib, P. K. Mascharak and N. Baidya, *Inorganic Chemistry*, 1991, **30**, 920-928.
10. J. K. Kowalska, A. W. Hahn, A. Albers, C. E. Schiewer, R. Bjornsson, F. A. Lima, F. Meyer and S. DeBeer, *Inorganic chemistry*, 2016, **55**, 4485-4497.
11. M. M. van Schooneveld and S. DeBeer, *Journal of Electron Spectroscopy and Related Phenomena*, 2015, **198**, 31-56.